Numerical finite element formulation of the Schapery non-linear viscoelastic material model

Rami M. Haj-Ali[*,†] and Anastasia H. Muliana

School of Civil and Environmental Engineering, Georgia Institute of Technology, Atlanta, GA 30332-0355, U.S.A.

SUMMARY

This study presents a numerical integration method for the non-linear viscoelastic behaviour of isotropic materials and structures. The Schapery's three-dimensional (3D) non-linear viscoelastic material model is integrated within a displacement-based finite element (FE) environment. The deviatoric and volumetric responses are decoupled and the strain vector is decomposed into instantaneous and hereditary parts. The hereditary strains are updated at the end of each time increment using a recursive formulation. The constitutive equations are expressed in an incremental form for each time step, assuming a constant incremental strain rate. A new iterative procedure with predictor–corrector type steps is combined with the recursive integration method. A general polynomial form for the parameters of the non-linear Schapery model is proposed. The consistent algorithmic tangent stiffness matrix is realized and used to enhance convergence and help achieve a correct convergent state. Verifications of the proposed numerical formulation are performed and compared with a previous work using experimental data for a glassy amorphous polymer PMMA. Copyright © 2003 John Wiley & Sons, Ltd.

KEY WORDS: viscoelastic; non-linear; Schapery; finite element; recursive; iterative

INTRODUCTION

Polymeric materials are widely used in many structural applications due to their flexible design and low weight. The behaviour of polymeric materials is usually time-dependent under combination of mechanical loading, temperature and moisture environment and damage evolution due to the above. Non-linear viscoelastic constitutive models have been proposed to model the complex non-linear mechanical behaviour of polymers.

The response of a linear viscoelastic material subject to complex loading history can be obtained from the solution of either an integral or a differential constitutive form. The Boltzmann convolution integral is usually used to represent the superposition principle that defines

---

[*]Correspondence to: Rami M. Haj-Ali, School of Civil and Environmental Engineering, Georgia Institute of Technology, Atlanta GA 30332-0355, U.S.A.
[†]E-mail: rami.haj-ali@ce.gatech.edu

the linear viscoelastic behaviour. Two common methods are often used to represent the uni-axial transient part of a viscoelastic response. Findley *et al.* [1] used a power law function to express the transient strain or time-dependent modulus of a material under constant stress. Non-linear and temperature effects can be modelled by having the power-law coefficients as functions of stress and temperature. A Prony exponential series is another mathematical form that is also used to represent the transient compliance or modulus of linear viscoelastic materials. The Prony series can be linked to the solution of a mechanical analogy of springs and dashpots (Kelvin and Maxwell arrangements) used to represent the instantaneous and transient responses of the material. The Prony series form is computationally convenient when used in recursive integration methods.

Schapery [2] used thermodynamics of irreversible processes to develop a single-integral constitutive model for non-linear viscoelastic materials. The non-linear viscoelastic parameters or functions can be determined from creep and recovery tests. Schapery's non-linear viscoelastic model has been extensively applied for isotropic and anisotropic materials. Numerical integration methods for non-linear viscoelastic constitutive models, within a finite element (FE) formulation, have been explored for both isotropic and anisotropic materials. Henriksen [3] used Schapery's non-linear constitutive model and developed a recursive numerical integration algorithm. A Prony exponential series is required to express the transient compliance in order to allow for a recursive form of the hereditary integral. The computer storage requirement for using this method is proportional to the number of terms in the Prony series, at each integration point. The non-linear viscoelastic behaviour considered was mainly due to higher stress magnitudes. FE analysis was performed for FM-73 adhesive systems under creep and recovery tests. Their results compared very well with the experimental data performed by Perez and Weitsman [4]. Roy and Reddy [5] used a similar integration approach to Henriksen's and formulated a numerical integration method for the Schapery non-linear viscoelastic model coupled with moisture sorption and used for 2D FE modelling of adhesively bonded joints. The non-linear viscoelastic parameters depend on stress and temperature. A coupled non-linear Fickean diffusion model is also used where its diffusion coefficient is a function of temperature, dilatational strain and stress, and moisture concentration. Lai and Bakker [6] modified Henriksen recursive algorithm in order to include non-linear effects due to temperature and physical aging that accounted for by using reduced time functions. Isotropic material was considered which allowed decoupling the deviatoric and volumetric parts. The constitutive formulation was used to model experimental tests with PMMA polymer. Taouti and Ceder-baum [7] presented a numerical scheme to obtain the non-linear stress relaxation response from the non-linear creep response in the form of discrete experimental data. An exponential (Prony) series was used for the transient creep compliance. Their method transformed the non-linear convolution integral into a system of first-order differential equations. Non-linear stress relaxation was predicted by solving these equations. Taouti and Cederbaum [8] extended this numerical procedure for the non-linear viscoelastic characterization and analysis of orthotropic laminated plates. Finally, Simo and Hughes [9] reviewed many topics on computational inelasticity including viscoelasticity. Irreversible thermodynamics with internal state variables was used to derive a general class of strain-based non-linear viscoelastic models. Attention was also given to integrating linear viscoelastic models within a non-linear geometric formulation.

Li [10] developed a FE procedure to analyse non-linear viscoelastic response for anisotropic solid materials subjected to mechanical and hygrothermal loads. A recursive algorithm is used to evaluate the hereditary integral. The time increment is assumed small and the stress varies

linearly over this short time period. The non-linear viscoelastic parameters are function of the current stresses. Therefore, the stiffness and compliance matrices depend on the current stress states. The hereditary stresses can be obtained from material properties, time increment, strains and stresses of the previous step. Poon and Ahmad [11] proposed an integration scheme for Schapery's integral expressed with strain-based non-linear functions and applied independently for each of the anisotropic moduli. This explicit constitutive form can be more suited for displacement-based FE environment because does not require a correction scheme. However, it is not clear how this model can be calibrated from experimental data for a general anisotropic behaviour. Yi *et al.* [12–14] developed a FE integration procedure to analyse non-linear viscoelastic response in laminated composites subjected to mechanical and hygrothermal loading. A lamina was modelled under generalized plane strain. A virtual work with small strain theory is used to derive the equilibrium equations. A recursive viscoelastic exponential series is generated from the time-domain integration of the virtual work with the non-linear constitutive model. The terms of the integration can be expressed as residual nodal vectors that are stored only for the previous increment. Different non-linear viscoelastic problems in laminated composites were solved using this FE method, such as interlaminar stress, bending and twisting of laminated composites.

This study deals with the numerical formulation of the Schapery type non-linear viscoelastic constitutive models. The formulation is carried out such that a constant incremental strain rate is assumed during each increment. This is suitable for displacement-based FE environment. A two-step numerical algorithm is proposed where recursive integration is carried out and followed by a predictor–corrector stress update to minimize a strain residual. A simple consistent tangent stiffness matrix is realized from the correction algorithm. The linearized stress update part of this study employs the numerical formulation previously derived by Taylor [15], Henriksen [3], and Lai and Bakker [6]. Finally, numerical recursive integration examples are given using the experimental data from Lai and Bakker [6] in order to examine the proposed numerical formulations.

NUMERICAL INTEGRATION ALGORITHM

A multiaxial non-linear viscoelastic constitutive model for isotropic materials is numerically derived using the Schapery [2] single integral constitutive model. The proposed numerical integration is suitable for a displacement based FE material-modelling environment. A recurrence numerical algorithm for linear viscoelastic integral has been proposed by Taylor *et al.* [15]. The convolution integral is divided into recursive parts. This allows the incremental formulation and integration for the current stress state from the history variables stored at the previous time step, and the current time and strain increments. The recursive approach tremendously minimizes the storage required to perform the constitutive integration. Henriksen [3], and Lai and Bakker [6] used a similar recursive algorithm for the non-linear constitutive integral. However, using the recurrence integration for the non-linear viscoelastic integrals requires additional assumptions on the non-linear functions and their variation over time increments. These are explicitly stated later in this section. In a general FE analysis, some of these assumptions may not be valid, especially when the non-linear viscoelastic integral is expressed in terms of stress-based variables. Therefore, an iterative scheme is required in order to minimize the error of the recurrence integration.

The current constitutive modelling approach modifies that of Lai and Bakker [6]. Additional non-linear and iterative formulation is needed to complete the integration of the non-linear viscoelastic model of Schapery. Furthermore, a consistent algorithmic tangent stiffness matrix is developed to enhance equilibrium and to help avoid misleading convergent states. A suggested general polynomial form for the non-linear parameters is proposed. Iterative correction algorithm is implemented and executed simultaneously at the constitutive level.

Uniaxial formulation

The Schapery uniaxial integral form for the current strain can be expressed by

$$\varepsilon^t \equiv \varepsilon(t) = g_0^{\sigma^t} D_0 \sigma^t + g_1^{\sigma^t} \int_0^t \Delta D^{(\psi^t - \psi^\tau)} \frac{\mathrm{d}(g_2^{\sigma^t}\sigma^\tau)}{\mathrm{d}\tau} \mathrm{d}\tau \tag{1}$$

where ψ is the reduced-time (effective time) given by

$$\psi^t \equiv \psi(t) = \int_0^t \frac{\mathrm{d}\xi}{a_\sigma^{\sigma^\xi} a_\mathrm{T}^\mathrm{T}} \tag{2}$$

The upper right superscript of a given term is used to denote an explicit variable. The non-linear material properties: g_0, g_1, g_2, and a_σ are also referred to herein as non-linear stress-functions because they depend only on stress variables, e.g. octahedral shear stress. These functions are always positive and equal to one for relatively small values of stress magnitudes (Boltzmann integral in linear viscoelasticity). The parameter a_σ acts as a time-scaling factor. The function a_T is a temperature dependent that is used to define a time scale shift factor for thermorheologically simple materials. The stress functions can also be temperature dependent, which makes Equation (1) represent the viscoelastic behaviour of a thermorheologically complex material. In addition to stress and temperature effects, moisture and physical aging effects can be included by adding their own time-scaling functions in Equation (2). The non-linear effects considered in this study are only due to stress.

The parameter g_0 is the non-linear instantaneous elastic compliance and measures the reduction or increase in stiffness. The transient creep parameter g_1 measures the non-linearity effect in the transient compliance. The parameter g_2 accounts for the load rate effect on the creep response. D_0 is the instantaneous uniaxial elastic compliance and ΔD is uniaxial transient compliance. The uniaxial transient compliance can be expressed using a Prony series as

$$\Delta D^{\psi^t} = \sum_{n=1}^{N} D_n(1 - \exp[-\lambda_n \psi^t]) \tag{3}$$

where N is the number of terms, D_n is the nth coefficient of the Prony series, and λ_n is the nth reciprocal of retardation time. Substituting Equation (3) into Equation (1) yields:

$$\varepsilon^t = g_0^t D_0 \sigma^t + g_1^t g_2^t \sum_{n=1}^{N} D_n - g_1^t \sum_{n=1}^{N} D_n q_n^t \tag{4}$$

where

$$q_n^t = \int_0^t \exp[-\lambda_n(\psi^t - \psi^\tau)] \frac{\mathrm{d}(g_2^\tau \sigma^\tau)}{\mathrm{d}\tau} \mathrm{d}\tau \tag{5}$$

A recursive integration form can be obtained from Equation (5) by dividing the integration into two parts. The first part includes the integral with limits $(0, t - \Delta t)$, i.e. up to the previous time step. The limits of the second part are taken as $(t - \Delta t, t)$, where t is the current time. Therefore,

$$q_n^t = \int_0^{t-\Delta t} \exp[-\lambda_n(\psi^t - \psi^\tau)] \frac{d(g_2^\tau \sigma^\tau)}{d\tau} \, d\tau + \int_{t-\Delta t}^t \exp[-\lambda_n(\psi^t - \psi^\tau)] \frac{d(g_2^\tau \sigma^\tau)}{d\tau} \, d\tau \qquad (6)$$

A reduced time increment is defined by

$$\Delta\psi^t \equiv \psi^t - \psi^{t-\Delta t} \qquad (7)$$

The first term of integral in Equation (6) can be expressed by the integral at $(t - \Delta t)$ and the current reduced time:

$$\int_0^{t-\Delta t} \exp[-\lambda_n(\psi^t - \psi^\tau)] \frac{d(g_2^\tau \sigma^\tau)}{d\tau} d\tau = \exp[-\lambda_n \Delta\psi^t] q_n^{t-\Delta t} \qquad (8)$$

The second integral of Equation (6) is carried out by parts while assuming that the term $(g_2^\tau \sigma^\tau)$ is linear over the current time step increment (Δt). In addition, it is assumed that the shift parameter as is not directly a function of time. Therefore, the second integral can be reduced to

$$\int_{t-\Delta t}^t \exp[-\lambda_n(\psi^t - \psi^\tau)] \frac{d(g_2^\tau \sigma^\tau)}{d\tau} \, d\tau = \frac{1 - \exp[-\lambda_n \Delta\psi^t]}{\lambda_n \Delta\psi^t} (g_2^t \sigma^t - g_2^{t-\Delta t} \sigma^{t-\Delta t}) \qquad (9)$$

The $q_n^{t-\Delta t}$ expression in Equation (8) is the hereditary integral for every term in the Prony series at the end of the previous time $(t - \Delta t)$. These can be considered as history variables that need to be updated and stored at the end of each time increment. Substitute Equations (8) and (9) into Equation (6), the hereditary integral can be written at the end of current time (t) as

$$q_n^t = \exp[-\lambda_n \Delta\psi^t] q_n^{t-\Delta t} + (g_2^t \sigma^t - g_2^{t-\Delta t} \sigma^{t-\Delta t}) \frac{1 - \exp[-\lambda_n \Delta\psi^t]}{\lambda_n \Delta\psi^t} \qquad (10)$$

The current total strain is obtained by rearranging and substituting Equation (10) into Equation (4):

$$\varepsilon^t = \left[g_0^t D_0 + g_1^t g_2^t \sum_{n=1}^N D_n - g_1^t g_2^t \sum_{n=1}^N D_n \frac{1 - \exp[-\lambda_n \Delta\psi^t]}{\lambda_n \Delta\psi^t} \right] \sigma^t$$

$$- g_1^t \sum_{n=1}^N D_n \left[\exp[-\lambda_n \Delta\psi^t] q_n^{t-\Delta t} - g_2^{t-\Delta t}(1 - \exp[-\lambda_n \Delta\psi^t]) \frac{\sigma^{t-\Delta t}}{\lambda_n \Delta\psi^t} \right]$$

$$\equiv \bar{D}^t \sigma^t - f^t \qquad (11)$$

Substituting Equation (10) into the second term in Equation (11), allows term f^t to be rewritten as

$$f^t = g_1^t \sum_{n=1}^N D_n \left[q_n^t - g_2^t \sigma^t \frac{1 - \exp[-\lambda_n \Delta\psi^t]}{\lambda_n \Delta\psi^t} \right] \qquad (12)$$

The above equation allows for the incremental strain–stress calculation for a time increment Δt, which is then added to the total stress or strain from the previous time step $(t - \Delta t)$. The incremental form of Equation (12) is expressed as

$$
\begin{aligned}
f^t - f^{t-\Delta t} &= g_1^t \sum_{n=1}^N D_n \left[q_n^t - g_2^t \sigma^t \frac{1 - \exp[-\lambda_n \Delta \psi^t]}{\lambda_n \Delta \psi^t} \right] \\
&\quad - g_1^{t-\Delta t} \sum_{n-1}^N D_n \left[q_n^{t-\Delta t} - g_2^{t-\Delta t} \sigma^{t-\Delta t} \frac{1 - \exp[-\lambda_n \Delta \psi^{t-\Delta t}]}{\lambda_n \Delta \psi^{t-\Delta t}} \right] \\
&= \sum_{n-1}^N D_n \left\{ (g_1^t \exp[-\lambda_n \Delta \psi^t] - g_1^{t-\Delta t}) q_n^{t-\Delta t} \right. \\
&\quad \left. + g_2^{t-\Delta t} \sigma^{t-\Delta t} \left(g_1^{t-\Delta t} \frac{1 - \exp[-\lambda_n \Delta \psi^{t-\Delta t}]}{\lambda_n \Delta \psi^{t-\Delta t}} - g_1^t \frac{1 - \exp[-\lambda_n \Delta \psi^t]}{\lambda_n \Delta \psi^t} \right) \right\}
\end{aligned}
$$

$$(13)$$

The current incremental strain is obtained by

$$
\begin{aligned}
\Delta \varepsilon^t &= \varepsilon^t - \varepsilon^{t-\Delta t} = (\bar{D}^t \sigma^t - \bar{D}^{t-\Delta t} \sigma^{t-\Delta t}) - (f^t - f^{t-\Delta t}) \\
&= \bar{D}^t \sigma^t - \bar{D}^{t-\Delta t} \sigma^{t-\Delta t} - \sum_{n=1}^N D_n (g_1^t \exp[-\lambda_n \Delta \psi^t] - g_1^{t-\Delta t}) q_n^{t-\Delta t} \\
&\quad - g_2^{t-\Delta t} \sum_{n=1}^N D_n \left[g_1^{t-\Delta t} \left(\frac{1 - \exp[-\lambda_n \Delta \psi^{t-\Delta t}]}{\lambda_n \Delta \psi^{t-\Delta t}} \right) - g_1^t \left(\frac{1 - \exp[-\lambda_n \Delta \psi^t]}{\lambda_n \Delta \psi^t} \right) \right] \sigma^{t-\Delta t}
\end{aligned}
$$

$$(14)$$

Multiaxial formulation

The previous numerical formulation for uniaxial viscoelastic behaviour is now used and generalized to derive multiaxial (3D) constitutive relations for isotropic materials. To that end, the deviatoric and volumetric strain–stress relations are decoupled. Stress components are chosen as the independent state variables. The formulation is carried out assuming the total strains are known for each time increment and the incremental strain rate is constant. This is consistent with many non-linear constitutive models implemented within a displacement-based finite element.

The Schapery integral constitutive model is applied twice for the deviatoric and volumetric strains as:

$$
e_{ij}^t = \frac{1}{2} g_0^t J_0 S_{ij}^t + \frac{1}{2} g_1^t \int_0^t \Delta J^{(\psi^t - \psi^\tau)} \frac{d(g_2^\tau S_{ij}^\tau)}{d\tau} \, d\tau
$$

$$(15)$$

$$
\varepsilon_{kk}^t = \frac{1}{3} g_0^t B_0 \sigma_{kk}^t + \frac{1}{3} g_1^t \int_0^t \Delta B^{(\psi^t - \psi^\tau)} \frac{d(g_2^\tau \sigma_{kk}^\tau)}{d\tau} \, d\tau
$$

$$(16)$$

Where e_{ij}, ε_{kk}, and S_{ij} are used to denote the deviatoric strains, volumetic strain, and the deviatoric stress, respectively. The non-linear parameters are assumed to be general polynomial functions of the effective octahedral shear stress. In this study, these functions are taken as

$$g_0 = 1 + \sum_{i=1}^{ng_0} \alpha_i \left\langle \frac{\bar{\sigma}}{\sigma_{\mathrm{o}}} - 1 \right\rangle^i, \quad g_1 = 1 + \sum_{i=1}^{ng_1} \beta_i \left\langle \frac{\bar{\sigma}}{\sigma_{\mathrm{o}}} - 1 \right\rangle^i$$

$$g_2 = 1 + \sum_{i=1}^{ng_2} \gamma_i \left\langle \frac{\bar{\sigma}}{\sigma_{\mathrm{o}}} - 1 \right\rangle^i, \quad a_\sigma = 1 \quad + \sum_{i=1}^{na\sigma} \delta_i \left\langle \frac{\bar{\sigma}}{\sigma_{\mathrm{o}}} - 1 \right\rangle^i \tag{17}$$

$$\psi^t = \frac{t}{a_\sigma}$$

where

$$\langle x \rangle = \begin{cases} x, & x > 0 \\ 0, & x \leqslant 0 \end{cases} \tag{18}$$

The coefficients $(\alpha_i, \beta_i, \gamma_i, \delta_i)$ can be calibrated from creep and recovery tests. The term σ_{o} is the effective stress limit that determines the end of the linear viscoelastic range. J_0 and B_0 are instantaneous elastic shear and bulk compliances, respectively. The terms ΔJ and ΔB are the transient shear and bulk compliances, respectively. It should be noted that the non-linear parameters can also depend on the mean stress. This has not been considered in this study; however, the present formulation can be easily generalized to include this functionality. Next, we further assume that the matrix Poisson ratio, v, is time independent. This allows expressing the two integrals in Equations (15) and (16) as a function of one hereditary integral:

$$\varepsilon_{ij}^t = e_{ij}^t + \frac{1}{3} \varepsilon_{kk}^t \delta_{ij}$$

$$= (1 + v) D_0 g_0^t S_{ij}^t + (1 + v) g_1^t \int_0^t \Delta D^{(\psi^t - \psi^\tau)} \frac{\mathrm{d}(g_2^\tau S_{ij}^\tau)}{\mathrm{d}\tau} \, \mathrm{d}\tau$$

$$+ \frac{(1 - 2v)}{3} \delta_{ij} \left[D_0 g_0^t \sigma_{kk}^t + g_1^t \int_0^t \Delta D^{(\psi^t - \psi^\tau)} \frac{\mathrm{d}(g_2^\tau \sigma_{kk}^t)}{\mathrm{d}\tau} \, \mathrm{d}\tau \right] \tag{19}$$

Comparing the terms in Equations (15) and (16) with those in Equation (19) yield:

$$J_0 = 2(1 + v) D_0 \qquad\qquad B_0 = 3(1 - 2v) D_0$$

$$\Delta J(\psi) = 2(1 + v) \Delta D(\psi) \qquad \Delta B(\psi) = 3(1 - 2v) \Delta D(\psi) \tag{20}$$

Next, the previous numerical result from the uniaxial integration in Equation (11) is used to provide recursive integration for Equations (15) and (16), respectively:

$$e_{ij}^t = \frac{1}{2} \left[g_0^t J_0 + g_1^t g_2^t \sum_{n=1}^N J_n - g_1^t g_2^t \sum_{n=1}^N J_n \frac{1 - \exp[-\lambda_n \Delta \psi^t]}{\lambda_n \Delta \psi^t} \right] S_{ij}^t$$

$$- \frac{1}{2} g_1^t \sum_{n=1}^{N} J_n \left[\exp[-\lambda_n \Delta \psi^t] q_{ij,n}^{t-\Delta t} - g_2^{t-\Delta t} \frac{1 - \exp[-\lambda_n \Delta \psi^t]}{\lambda_n \Delta \psi^t} S_{ij}^{t-\Delta t} \right]$$

$$\equiv \bar{J}^t S_{ij}^t - d_{ij}^t \tag{21}$$

$$\varepsilon_{kk}^t = \frac{1}{3} \left[g_0^t B_0 + g_1^t g_2^t \sum_{n=1}^{N} B_n - g_1^t g_2^t \sum_{n=1}^{N} B_n \frac{1 - \exp[-\lambda_n \Delta \psi^t]}{\lambda_n \Delta \psi^t} \right] \sigma_{kk}^t$$

$$- \frac{1}{3} g_1^t \sum_{n=1}^{N} B_n \left[\exp[-\lambda_n \Delta \psi^t] q_{kk,n}^{t-\Delta t} - g_2^{t-\Delta t} \frac{1 - \exp[-\lambda_n \Delta \psi^t]}{\lambda_n \Delta \psi^t} \sigma_{kk}^{t-\Delta t} \right]$$

$$\equiv \bar{B}^t \sigma_{kk}^t - V_{kk}^t \tag{22}$$

The terms $q_{ij,n}^{t-\Delta t}$ and $q_{kk,n}^{t-\Delta t}$ are the shear and volumetric hereditary integrals for every term in the Prony series, expressed at the end of previous time increment $(t - \Delta t)$.

Equations (21) and (22) are used with some algebraic manipulations to derive expressions for the incremental deviatoric and volumetric strains. The results are written as

$$\Delta e_{ij}^t = e_{ij}^t - e_{ij}^{t-\Delta t}$$

$$= \bar{J}^t S_{ij}^t - \bar{J}^{t-\Delta t} S_{ij}^{t-\Delta t} - \frac{1}{2} \sum_{n=1}^{N} J_n (g_1^t \exp[-\lambda_n \Delta \psi^t] - g_1^{t-\Delta t}) q_{ij,n}^{t-\Delta t}$$

$$- \frac{1}{2} g_2^{t-\Delta t} \sum_{n=1}^{N} J_n \left[g_1^{t-\Delta t} \left(\frac{1 - \exp[-\lambda_n \Delta \psi^{t-\Delta t}]}{\lambda_n \Delta \psi^{t-\Delta t}} \right) - g_1^t \left(\frac{1 - \exp[-\lambda_n \Delta \psi^t]}{\lambda_n \Delta \psi^t} \right) \right] S_{ij}^{t-\Delta t} \tag{23}$$

$$\Delta \varepsilon_{kk}^t = \varepsilon_{kk}^t - \varepsilon_{kk}^{t-\Delta t}$$

$$= \bar{B}^t \sigma_{kk}^t - \bar{B}^{t-\Delta t} \sigma_{kk}^{t-\Delta t} - \frac{1}{3} \sum_{n=1}^{N} B_n (g_1^t \exp[-\lambda_n \Delta \psi^t] - g_1^{t-\Delta t}) q_{kk,n}^{t-\Delta t}$$

$$- \frac{1}{3} g_2^{t-\Delta t} \sum_{n=1}^{N} B_n \left[g_1^{t-\Delta t} \left(\frac{1 - \exp[-\lambda_n \Delta \psi^{t-\Delta t}]}{\lambda_n \Delta \psi^{t-\Delta t}} \right) - g_1^t \left(\frac{1 - \exp[-\lambda_n \Delta \psi^t]}{\lambda_n \Delta \psi^t} \right) \right] \sigma_{kk}^{t-\Delta t} \tag{24}$$

The above equations can be used to determine the unknown stress increment for a given strain increment and the previous history state, $q_{ij,n}^{t-\Delta t}$ and $q_{kk,n}^{t-\Delta t}$, $n = 1..N$. The problem is that the non-linear stress functions are not known at the current time (t). Therefore, an iterative method is needed in order to find the correct stress states. To that end, Equations (23) and (24) are further linearized using the following approximations:

$$g_\alpha^t = g_\alpha^{t-\Delta t}, \quad \alpha = 0, 1, 2$$
$$\Delta \psi^t = \Delta \psi^{t-\Delta t} \tag{25}$$

This allows generating expressions for the approximate or trial incremental stresses:

$$\Delta S_{ij}^{t,\mathrm{tr}} = \frac{1}{\bar{J}^{t,\mathrm{tr}}} \left[\Delta e_{ij}^t + \frac{1}{2}\, g_1^{t,\mathrm{tr}} \sum_{n=1}^{N} J_n(\exp[-\lambda_n \Delta\psi^t] - 1) q_{ij,n}^{t-\Delta t} \right] \tag{26}$$

$$\Delta \sigma_{kk}^{t,\mathrm{tr}} = \frac{1}{\bar{B}^{t,\mathrm{tr}}} \left[\Delta \varepsilon_{kk}^t + \frac{1}{3}\, g_1^{t,\mathrm{tr}} \sum_{n=1}^{N} B_n(\exp[-\lambda_n \Delta\psi^t] - 1) q_{kk,n}^{t-\Delta t} \right] \tag{27}$$

The terms $\bar{J}^{t,\mathrm{tr}}$ and $\bar{B}^{t,\mathrm{tr}}$ have the same form as in Equations (21) and (22), respectively, but with the non-linear parameters (g_0, g_1, g_2, and a_σ) are functions of the trial effective stress. Equations (26) and (27) are identical to the linearized relations developed by Lai and Bakker [6].

In this study an iterative scheme is developed in order to arrive at the correct stress state for a given strain increment. Otherwise, the strain and time increments may have to be very small in order to maintain accurate stress updates and minimize the errors due to the approximations in Equation (25). An iterative scheme is developed by defining strain residuals. These residual equations can be defined by using either the incremental strains, Equations (23) and (24), or the total strains, Equations (21) and (22), respectively. The equations are combined to form the residual strain errors in the form:

$$R_{ij}^t = \Delta e_{ij}^t + \frac{1}{3}\,\Delta \varepsilon_{kk}^t \delta_{ij} - \Delta \varepsilon_{ij}^t$$

$$= \bar{J}^t \sigma_{ij}^t + \frac{1}{3}(\bar{B}^t - \bar{J}^t)\sigma_{kk}^t \delta_{ij} - \bar{J}^{t-\Delta t}\sigma_{ij}^{t-\Delta t} - \frac{1}{3}(\bar{B}^{t-\Delta t} - \bar{J}^{t-\Delta t})\sigma_{ij}^{t-\Delta t}\delta_{ij}$$

$$- \left\{ \frac{1}{2}\sum_{n=1}^{N} J_n(g_1^t \exp[-\lambda_n\Delta\psi^t] - g_1^{t-\Delta t})q_{ij,n}^{t-\Delta t} \right.$$

$$+ \frac{1}{9}\left[\sum_{n=1}^{N} B_n(g_1^t \exp[-\lambda_n\Delta\psi^t] - g_1^{t-\Delta t})q_{kk,n}^{t-\Delta t} \right]\delta_{ij}$$

$$+ \frac{1}{2}\,g_2^{t-\Delta t}\sum_{n=1}^{N} J_n\left[g_1^{t-\Delta t}\left(\frac{1 - \exp[-\lambda_n\Delta\psi^{t-\Delta t}]}{\lambda_n\Delta\psi^{t-\Delta t}} \right) - g_1^t\left(\frac{1 - \exp[-\lambda_n\Delta\psi^t]}{\lambda_n\Delta\psi^t} \right) \right]S_{ij}^{t-\Delta t}$$

$$+ \frac{1}{9}\,g_2^{t-\Delta t}\sum_{n=1}^{N} B_n\left[g_1^{t-\Delta t}\left(\frac{1 - \exp[-\lambda_n\Delta\psi^{t-\Delta t}]}{\lambda_n\Delta\psi^{t-\Delta t}} \right) \right.$$

$$\left.\left. - g_1^t\left(\frac{1 - \exp[-\lambda_n\Delta\psi^t]}{\lambda_n\Delta\psi^t} \right) \right]\delta_{ij}\sigma_{kk}^{t-\Delta t} \right\} \tag{28}$$

A Jacobian matrix is formed by taking the derivative of the residual tensor with respect to the incremental stress as

$$\frac{\partial R_{ij}^t}{\partial \sigma_{kl}^t} = \bar{J}^t \delta_{ik}\delta_{jl} + \frac{1}{3}(\bar{B}^t - \bar{J}^t)\delta_{ij}\delta_{kl}$$

$$+ \frac{\partial \Delta \bar{\sigma}^t}{\partial \sigma_{kl}^t} \left\{ \frac{\partial \bar{J}^t}{\partial \Delta \bar{\sigma}^t} \sigma_{ij}^t + \frac{1}{3} \left(\frac{\partial \bar{B}^t}{\partial \Delta \bar{\sigma}^t} - \frac{\partial \bar{J}^t}{\partial \Delta \bar{\sigma}^t} \right) \sigma_{kk}^t \delta_{ij} \right.$$

$$- \frac{1}{2} \frac{\partial g_1^t}{\partial \Delta \bar{\sigma}^t} \sum_{n=1}^N J_n \left[\exp[-\lambda_n \Delta \psi^t] q_{ij,n}^{t-\Delta t} - g_2^{t-\Delta t} \left(\frac{1 - \exp[-\lambda_n \Delta \psi^t]}{\lambda_n \Delta \psi^t} \right) S_{ij}^{t-\Delta t} \right]$$

$$- \frac{1}{2} \frac{\partial a_\sigma^t}{\partial \Delta \bar{\sigma}^t} g_1^t \sum_{n=1}^N J_n \left[\exp[-\lambda_n \Delta \psi^t] \left(\frac{\lambda_n \Delta t q_{ij,n}^{t-\Delta t}}{a_\sigma^{t2}} + \frac{S_{ij}^{t-\Delta t}}{a_\sigma^t} \right) \right.$$

$$\left. - g_2^{t-\Delta t} \left(\frac{1 - \exp[-\lambda_n \Delta \psi^t]}{\lambda_n \Delta \psi^t} \right) S_{ij}^{t-\Delta t} \right]$$

$$- \frac{1}{9} \frac{\partial g_1^t}{\partial \Delta \bar{\sigma}^t} \sum_{n=1}^N B_n \left[\exp[-\lambda_n \Delta \psi^t] q_{kk,n}^{t-\Delta t} - g_2^{t-\Delta t} \left(\frac{1 - \exp[-\lambda_n \Delta \psi^t]}{\lambda_n \Delta \psi^t} \right) \sigma_{kk}^{t-\Delta t} \right] \delta_{ij}$$

$$- \frac{1}{9} \frac{\partial a_\sigma^t}{\partial \Delta \bar{\sigma}^t} g_1^t \sum_{n=1}^N B_n \left[\exp[-\lambda_n \Delta \psi^t] \left(\frac{\lambda_n \Delta t \, q_{kk,n}^{t-\Delta t}}{a_\sigma^{t2}} + \frac{\sigma_{kk}^{t-\Delta t}}{a_\sigma^t} \right) \right.$$

$$\left. \left. - g_2^{t-\Delta t} \left(\frac{1 - \exp[-\lambda_n \Delta \psi^t]}{\lambda_n \Delta \psi^t} \right) \sigma_{kk}^{t-\Delta t} \right] \delta_{ij} \right\} \tag{29}$$

where

$$\frac{\partial \Delta \bar{\sigma}^t}{\partial \sigma_{kl}^t} = \frac{3}{2} \frac{S_{ij}^t}{\Delta \bar{\sigma}^t} \left(\delta_{ij} \delta_{jl} - \frac{1}{3} \delta_{ij} \delta_{kl} \right)$$

Linearization of the residual allows forming a system of linear equation that can be solved for an updated trial stress that is used iteratively until a satisfied level of residual norm can be tolerated. Once convergence is achieved, the hereditary integrals in each prony series are calculated and stored in order to be used in the next time integration step. These are:

$$q_{ij,n}^t = \exp[-\lambda_n \Delta \psi^t] q_{ij,n}^{t-\Delta t} + (g_2^t S_{ij}^t - g_2^{t-\Delta t} S_{ij}^{t-\Delta t}) \frac{1 - \exp[-\lambda_n \Delta \psi^t]}{\lambda_n \Delta \psi^t} \tag{30}$$

$$q_{kk,n}^t = \exp[-\lambda_n \Delta \psi^t] q_{kk,n}^{t-\Delta t} + (g_2^t \sigma_{kk}^t - g_2^{t-\Delta t} \sigma_{kk}^{t-\Delta t}) \frac{1 - \exp[-\lambda_n \Delta \psi^t]}{\lambda_n \Delta \psi^t} \tag{31}$$

Next, we can define a consistent tangent compliance by taking the partial derivative of the incremental strain with respect to the incremental stress at the end of the current time step. Using Equation (29), one can realize the consistent tangent compliance matrix, $\dot{S}_{ijkl}^t$, at the converged state, as

$$\dot{S}_{ijkl}^t \equiv \frac{\partial \Delta \varepsilon_{ij}^t}{\partial \Delta \sigma_{kl}^t} = \frac{\partial R_{ij}^t}{\partial \Delta \sigma_{kl}^t}, \quad \|R_{ij}^t\| \to 0 \tag{32}$$

Table I. Elastic compliance and Prony series coeffi-
cients for the PMMA polymer.

n	λ_n (s^{-1})	$D_n \times 10^{-6}$ (MPa^{-1})
1	1	23.6358
2	10^{-1}	5.6602
3	10^{-2}	14.8405
4	10^{-3}	18.8848
5	10^{-4}	28.5848
6	10^{-5}	40.0569
7	10^{-6}	60.4235
8	10^{-7}	79.6477
9	10^{-8}	162.1790
D_0	270.9×10^{-6} (MPa^{-1})	

NUMERICAL IMPLEMENTATION AND VERIFICATION

The proposed numerical constitutive model is implemented within a displacement-based FE code. The material subroutine (UMAT) of the ABAQUS FE code [16] is used for this purpose. The 3D-viscoelastic response is generated at each material point (Gaussian integration points). Calibration and verification of the proposed numerical model are performed with test results on glassy amorphous polymer material (PMMA) reported by Lai and Bakker [6]. The calibrated elastic compliance and Prony parameters are given in Table I. The polynomial stress-dependent non-linear functions in the Schapery equation are determined from the experimental test, as shown in Figure 1. Fourth-order polynomials, Equation (17) are sufficient in calibrating the non-linear stress-dependent parameters. The effective stress (σ_o) that determines the limit of the linear response is 20 MPa. The polynomial coefficients are calibrated from the experimental data where the range of the effective stress is 0–40 MPa. The accuracy of these polynomial functions is within this range; beyond this stress level the polynomial functions may not represent the actual behaviour of the material. The calibrated polynomial coefficients for the four non-linear parameters are shown in Figure 1.

In order to simulate a stress step function in a creep test, a parametric study is carried to examine the effect of using different initial time increments on the instantaneous material response with varying stress levels. This is important in order to determine the range of initial time increment that can be used to simulate a Heaviside step function. Total strain values are reported for different time-increment sizes and compared with the analytical solution for several load levels (10–40 MPa), as shown in Figure 2. The initial time increment size can affect the accuracy of the results and a large time increment may lead to a diverged solution. The divergence from the elastic response occurs either with increasing applied stress levels or with large initial time increments. As a result, it is concluded that an initial time increment can be chosen in the range: 10^{-5}–10^{-2} s in order to represent an instantaneous response for this material.

A second parametric study is performed to examine the constitutive-level strain residuals generated during the iterations of a given time increment. Figures 3 and 4 show the strain
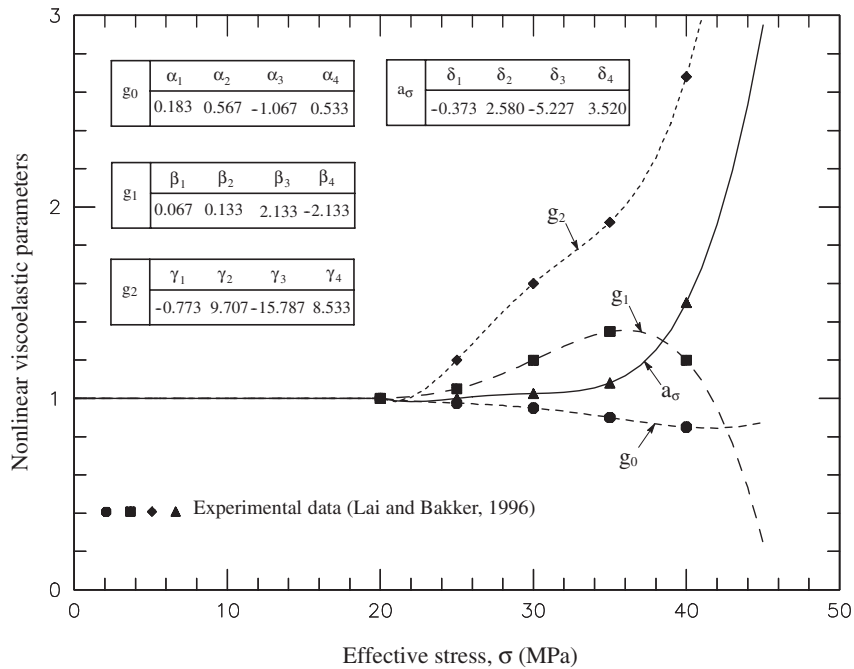
Figure 1. Non-linear stress-dependent parameters in the Schapery's equations for PMMA polymer.

residuals during the iteration process for creep analyses under two applied stresses of 35 and 40 MPa, respectively. It is seen from the initial residuals that using a linearized stress-update alone usually leads to a large residual strain, an error of more than 5% in our case. The proposed iterative procedure is needed in order to minimize this error. Similar convergence behaviour is shown in Figure 4 for the analysis with applied stress of 40 MPa. Convergence problems occurred during or at the beginning of the cases where applied stresses are equal or exceed the 40 MPa. This is because the non-linear functions were calibrated up to the 40 MPa stress magnitude, as shown in Figure 1. Convergence is also not guaranteed beyond this stress level because some of the non-linear functions have rapidly changing values and approach asymptotic levels. This will slow convergence and often lead to divergence.

The experimental data from Lai and Bakker [6] are now used to verify the proposed numerical modelling algorithm. A series of tensile creep test for 30 min followed by recovery test for 2 h were conducted under several stress level (15–35 MPa) at room temperature. It was shown that the linear response occurs below 20 MPa. Predicted creep and recovery curves are shown in Figures 5 and 6, respectively. The numerical results, solid lines, match very well the test results, dashed lines. Figure 7 illustrates the same results as those in Figure 5 with added results from creep simulations using recursive-only model. This is done to compare the proposed recursive-iterative model with the results using a predictor-only scheme at the material level. Both cases include the same correction scheme at the element level. It is interesting to note that the 'global' iterative residual correction is not sufficient to reduce the error at the element level with increasing applied stress. Another numerical prediction of uniaxial response is also performed. Two-step creep loading for PMMA polymer is shown in
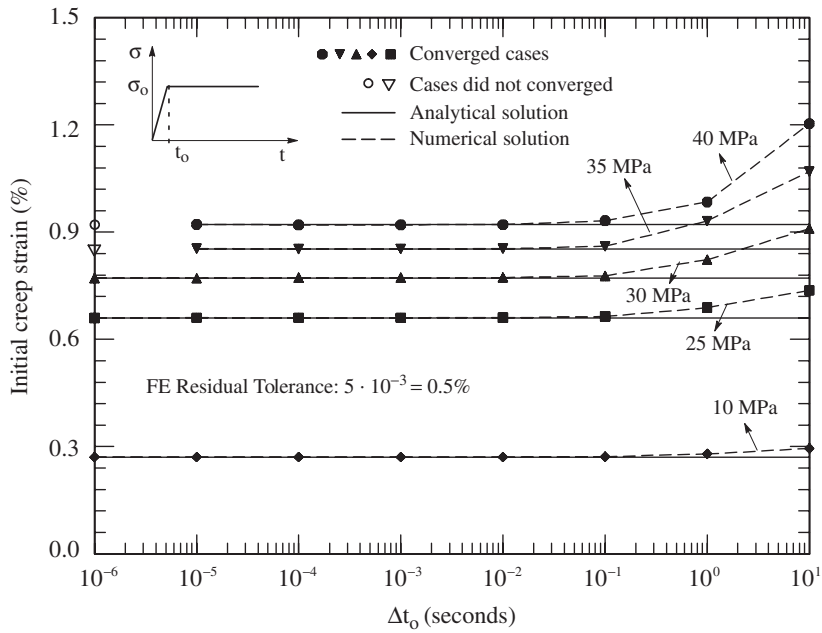
Figure 2. Effect of the time-increment size in the instantaneous static analysis for PMMA polymer.
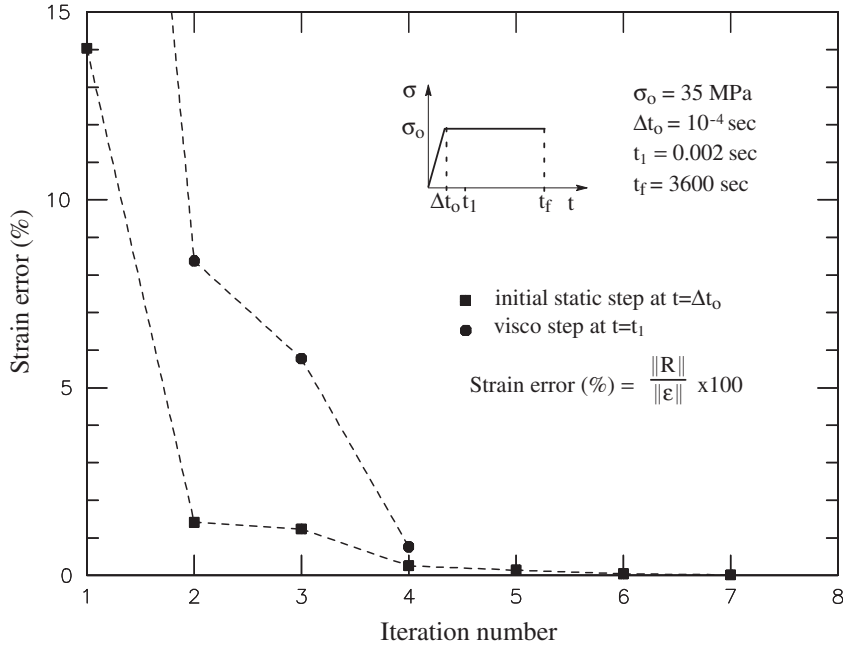

Figure 3. Residual strain for different time increments in an element under constant stress of 35 MPa.
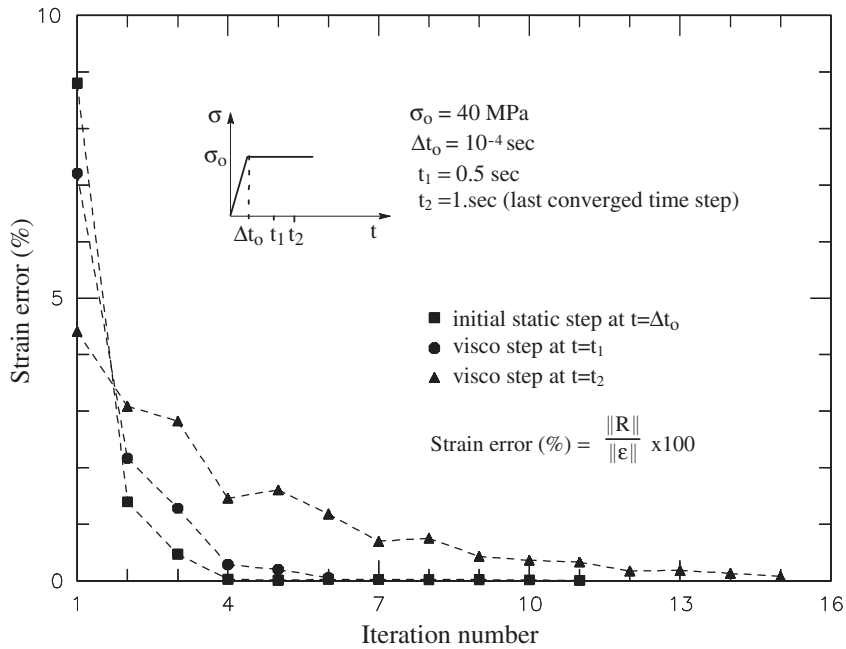
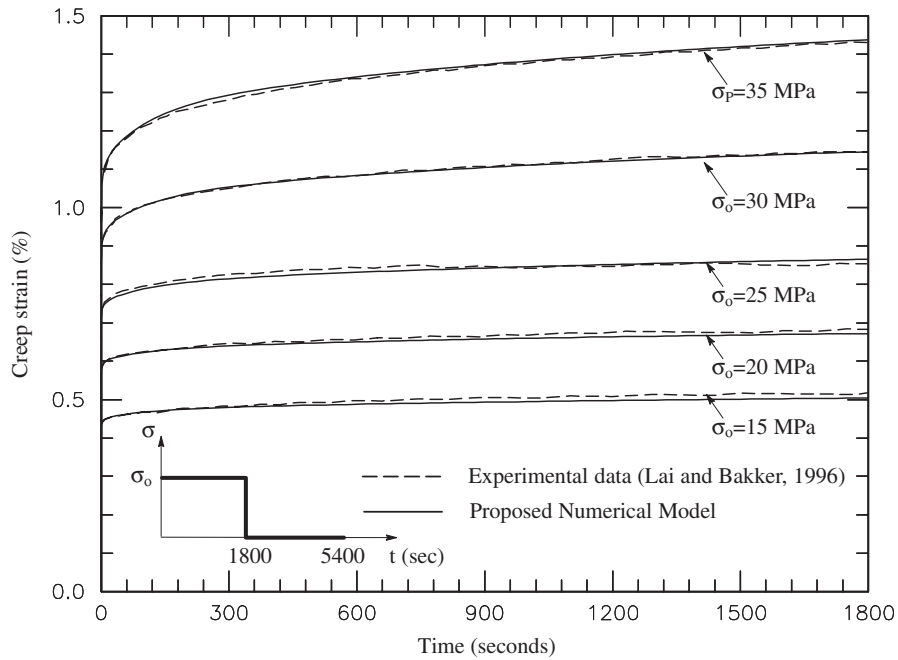Figure 4. Residual strain for different time increment in an element under constant stress of 40 MPa.
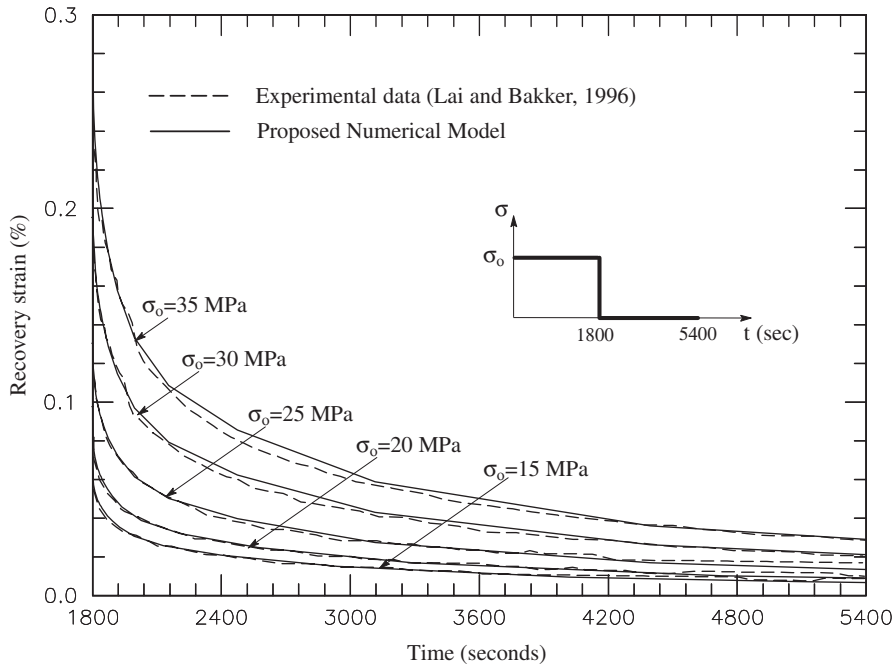

Figure 5. Creep strain response of PMMA.
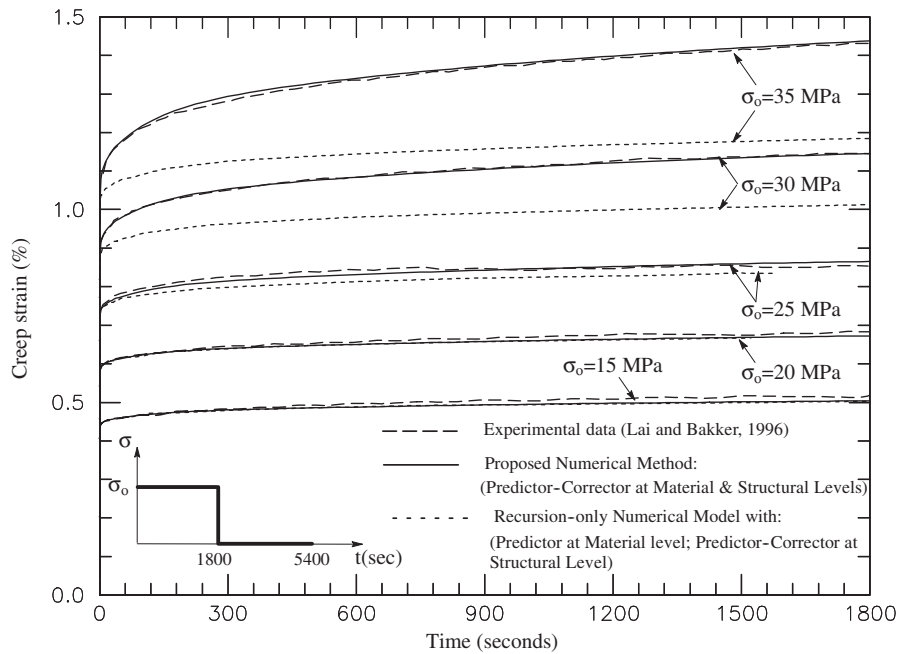
Figure 6. Recovery strain response of PMMA.

Figure 7. Creep strain response of PMMA using recursive-only model compared with the proposed recursive-iterative model (both models include the same correction scheme at the element level).
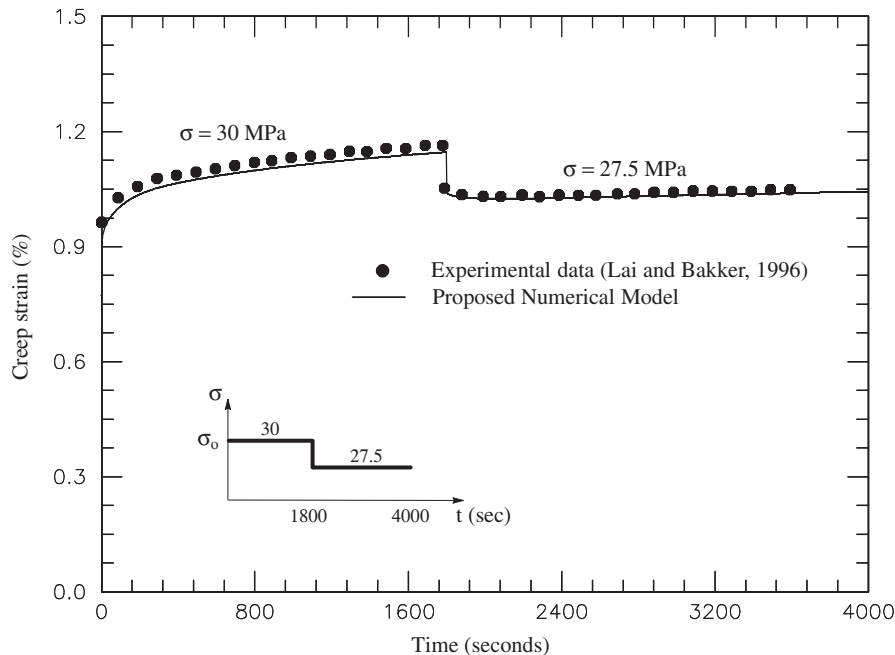
Figure 8. Two-step creep response for PMMA.

Figure 8. The prediction from the proposed numerical method is in good agreement with the experimental data.

The application of the proposed numerical algorithm for multiaxial response is presented using a FE model of a notched plate specimen under plane stress condition. The configuration of the rectangular plate follows the one of Lai and Bakker [6] with the dimensions of 800 mm × 400 mm and a hole radius of 20 mm. Owing to the double symmetric condition, only a quarter of the plate is modelled. A 20-node brick element with reduced integration is used for the analyses. One element is used through the thickness of 1 mm.

Two analyses were performed for the notched plate. The first analysis is a stress relaxation type where the plate is subjected to a uniform remote strain of 0.36% for duration of 10^6 s. Figure 9 shows the contours of strain error and number of iterations to convergence at various time steps (10^{-5}, 20, 1020, and 10^6 s). Initial residual strain at different times can have a magnitude of 0.15% or more. This is caused by the linearized approximation. As time increases, the accumulation of error at the converged stress states also increases. However, the iterative algorithm accomplishes the correct stress state and reduces the magnitude of strain error below 0.1% within 8 or less iterations. The stress relaxation response at three different locations is shown in Figure 10. At the edge of the hole, the stress magnitude is 37 MPa and a high non-linear response is shown. While at the distance away from the edge, the stresses are in the linear viscoelastic range. Therefore, the residual strains and number of iterations are less than those at the other locations, as seen in Figure 9. Figure 11 shows the spatial distribution of the axial-stress relaxation along the symmetry line, for short, intermediate, and long times.
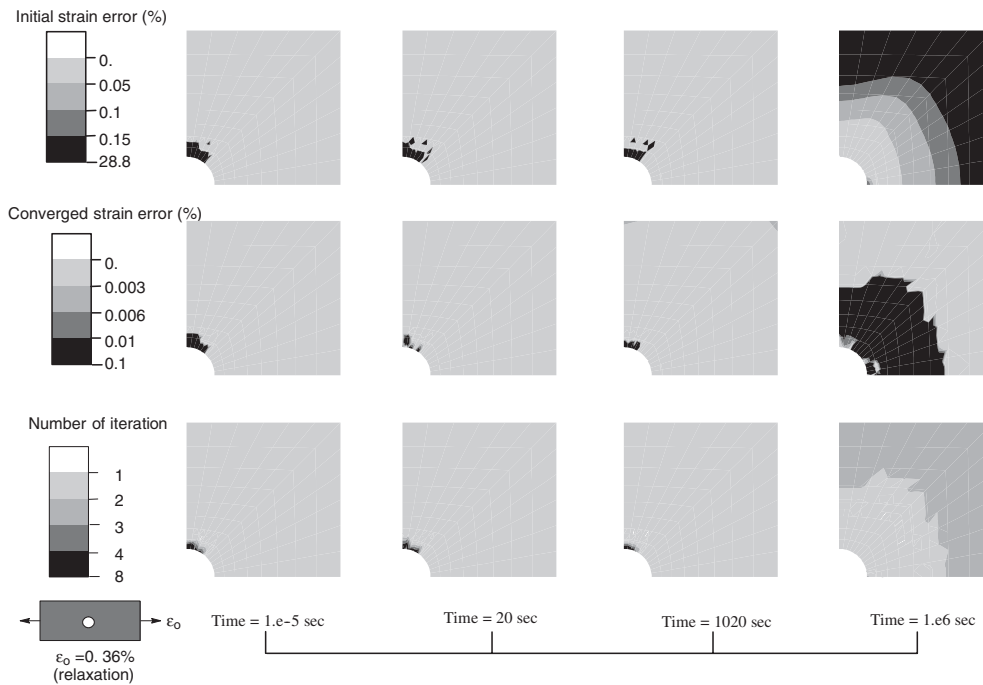
Figure 9. Contours of residual strain and number of iteration for notched
plate FE model under stress relaxation.

The second FE analysis is a creep type where the notched plate is subjected to a uniform remote stress of 13.5 MPa for duration of 10^6 s. The stress distributions along the mid-section of the plate, at times 10^{-5}, 1020, and 10^6 s, are shown in Figure 12. It is shown that the stress distribution changes with time when the large non-linearity occurs. While in the relatively low non-linear or linear visoelastic range, the stress distribution does not change with time. The contours of strain error and number of iterations at various times (10^{-5}, 20, 1020, and 10^6 s) are shown in Figure 13. The linearized approximation causes large residual strain, as indicated by the large initial residual strain (0.15% or more). The iterative procedure reduces the magnitude of strain error until it reaches a norm value below the 0.1% level. The creep strain response at three different locations is shown in Figure 14. The maximum strain occurs at the hole edge. Figure 15 shows the spatial distribution of the axial creep strain along the symmetry line, for short, intermediate, and long times.

CONCLUSIONS

A computational method is developed for the numerical integration of the Schapery-type non-linear viscoelastic material models with stress-based state variables. Previously developed recursive integration along with an iterative scheme to satisfy the constitutive residuals are shown as effective in modelling the viscoelastic behaviour of isotropic materials. The algorithm
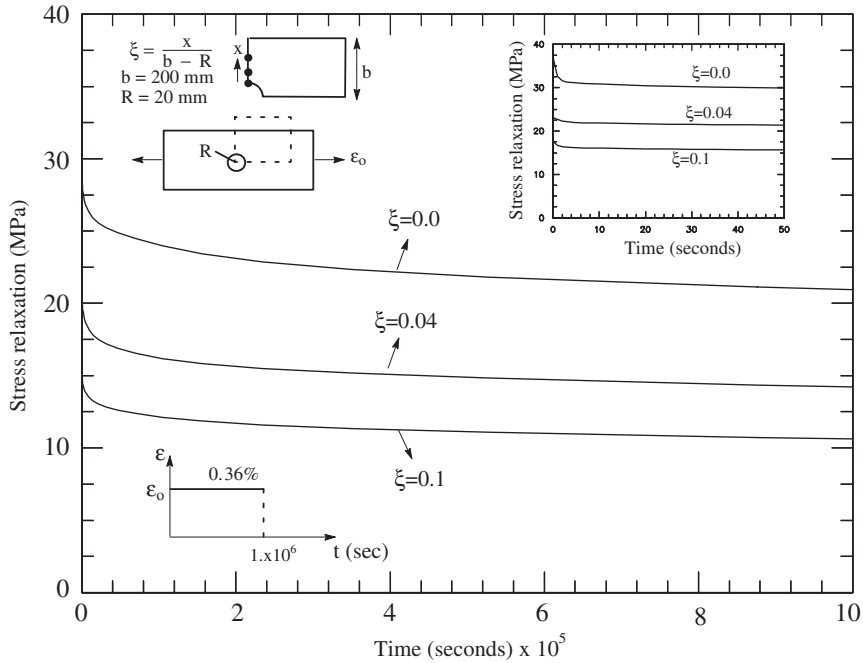
Figure 10. Stress relaxation at three points on a notched plate under tensile remote strain of 0.36%.
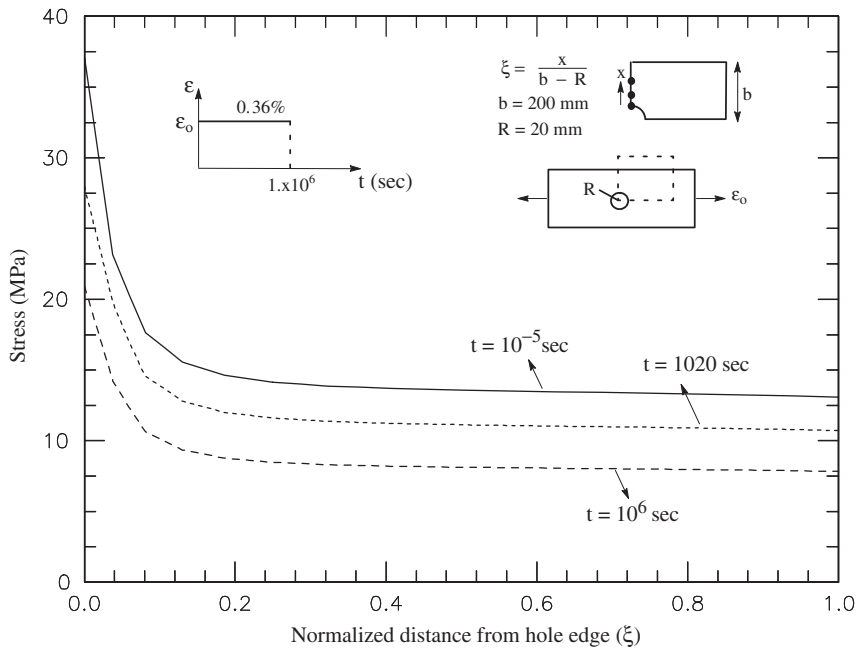
Figure 11. Stress distribution at the centre of a notched plate under tensile remote strain 0.36%.
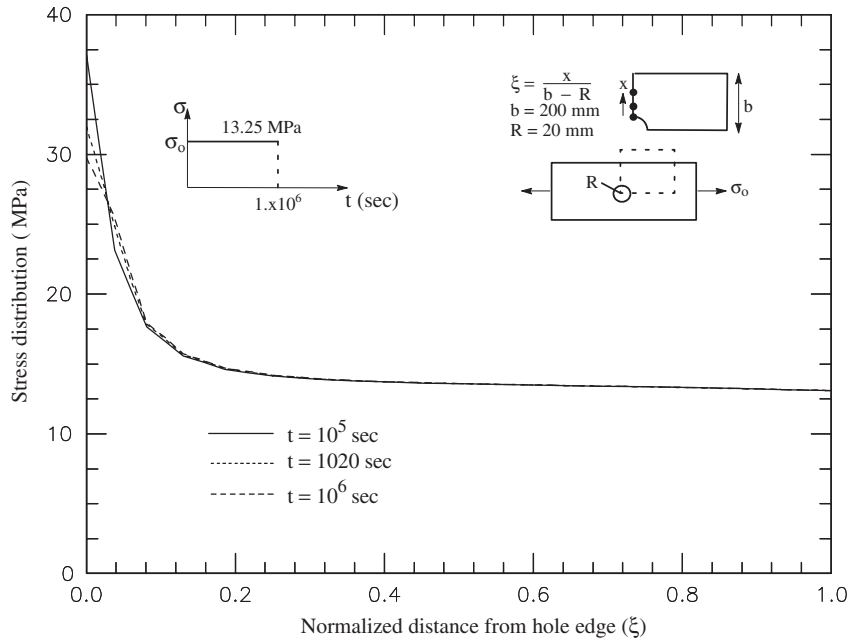
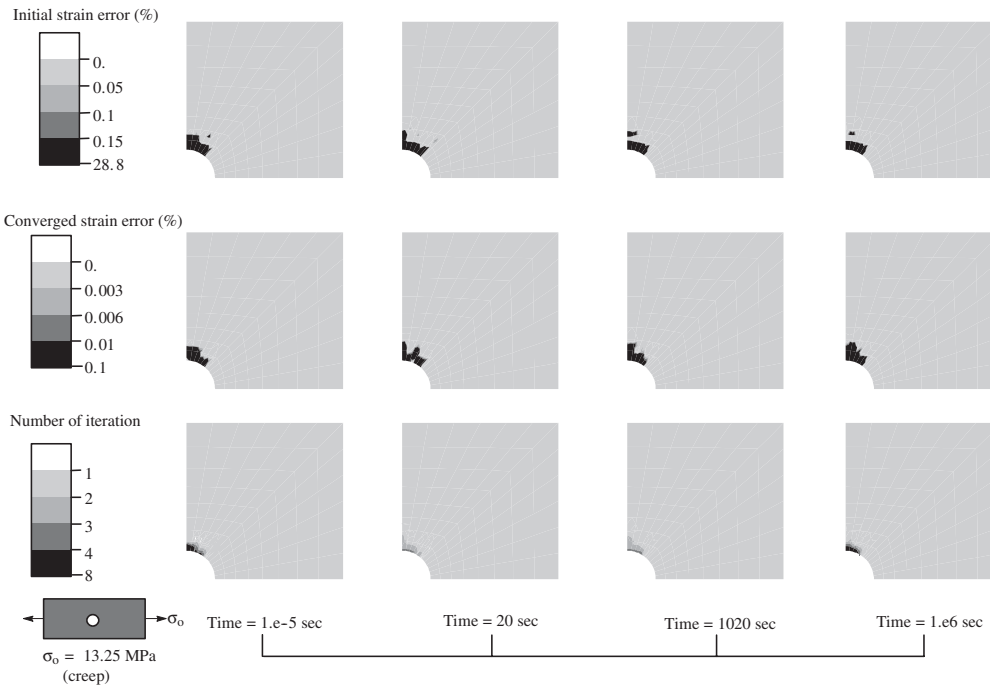Figure 12. Stress distribution for notched plate at different time.

Figure 13. Contours of residual strain and number of iteration
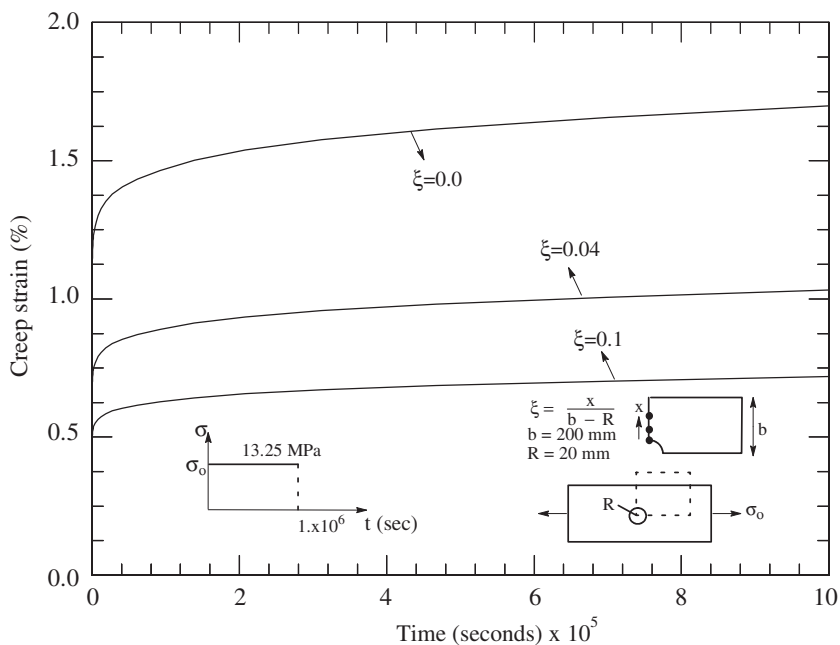for notched plate model under creep response.

Figure 14. Creep strain at three points on a notched plate subjected to tensile remote stress of 13.5 MPa.
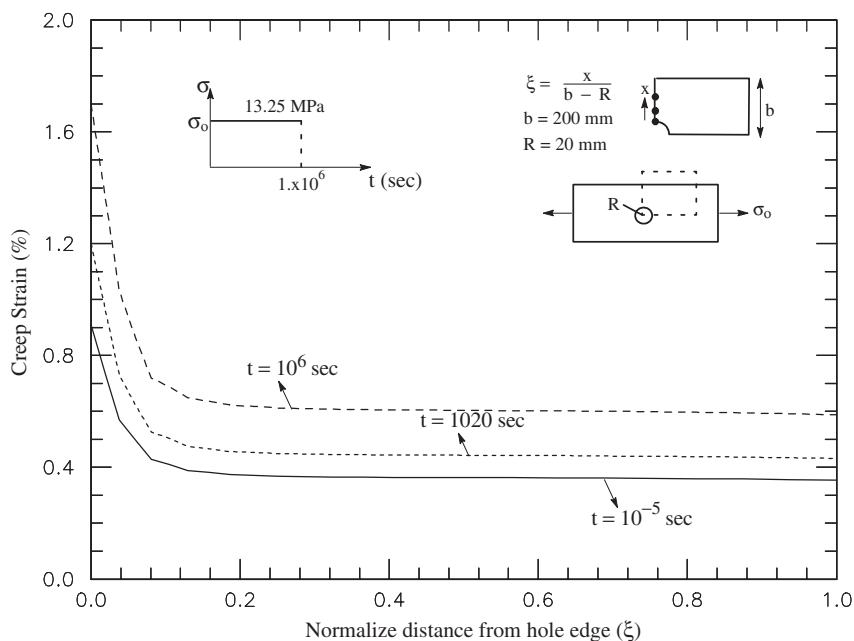

Figure 15. Strain distribution at the centre of a notched plate under tensile remote stress 13.5 MPa.

tangent stiffness is easily identified. Numerical examples are presented and compared with the experimental data of Lai and Bakker [6]. The constitutive model is implemented in a displacement-based FE code and results from numerical simulations are reported.

REFERENCES

1. Findley WN, Lai JS, Onaran K. *Creep and Relaxation of Non-linear Viscoelastic Materials*. Dover Publication: New York, 1976.
2. Schapery RA. On the characterization of non-linear viscoelastic materials. *Polymer Engineering and Science* 1969; **9**(4):295–310.
3. Henriksen M. Nonlinear viscoelastic stress analysis—a finite element approach. *Computers and Structures* 1984; **18**(1):133–139.
4. Peretz D, Weitsman Y. The non-linear thermo-viscoelastic characterization of FM-73 adhesives. *Journal of Rheology* 1983; **26**:245–261.
5. Roy S, Reddy JN. A finite element analysis of adhesively bonded composite joints with moisture diffusion and delayed failure. *Computers and Structures* 1988; **29**(6):1011–1031.
6. Lai J, Bakker A. 3-D Schapery representation for non-linear viscoelasticity and finite element implementation. *Computational Mechanics* 1996; **18**:182–191.
7. Touati D, Cederbaum G. On the prediction of stress relaxation from known creep of non-linear materials. *Journal of Engineering Materials and Technology* (ASME) 1997; **119**:121–124.
8. Touati D, Cederbaum G. Post buckling of non-linear viscoelastic imperfect laminated plates part I: material considerations. *Composite Structures* 1998; **42**:33–41.
9. Simo JC, Hughes TJR. *Computational Inelasticity*. Springer: New York, 1998.
10. Li R. Non-linear viscoelastic stress and fracture analyses of laminated composites. *Ph.D. Dissertation*, University of Washington, 1997.
11. Poon H, Ahmad F. A finite element constitutive update scheme for anisotropic, viscoelastic solids exhibiting non-linearity of the Schapery type. *International Journal for Numerical Methods in Engineering* 1998; **46**: 2027–2041.
12. Yi S, Hilton HH, Ahmad MF. Non-linear thermo-viscoelastic analysis of interlaminar stresses in laminated composites. *Journal of Applied Mechanics* (ASME) 1996; **63**:218–224.
13. Yi S. Finite element analysis of free edge stresses in non-linear viscoelastic composites under uniaxial extension, bending, and twisting loadings. *International Journal for Numerical Methods in Engineering* 1997; **40**: 4225–4238.
14. Yi S, Ahmad MF, Hilton HH. Non-linear viscoelastic stress singularities near free edges of unsymmetrically laminated composites. *International Journal of Solids and Structures* 1998; **35**(24): 3221–3237.
15. Taylor RL, Pister KS, Goudreau GL. Thermomechanical analysis of viscoelastic solids. *International Journal for Numerical Methods in Engineering* 1970; **2**:45–59.
16. ABAQUS, *User's Manual 5.8.* Hibbitt, Karlsson and Sorensen, Inc: Pawtucket, U.S.A., 1999.